

# Optimal Base Station Antenna Downtilt in Downlink Cellular Networks

Junnan Yang<sup>1</sup>, Student Member, IEEE, Ming Ding<sup>2</sup>, Senior Member, IEEE, Guoqiang Mao<sup>3</sup>, Fellow, IEEE, Zihuai Lin<sup>4</sup>, Senior Member, IEEE, De-Gan Zhang<sup>5</sup>, Member, IEEE, and Tom H. Luan<sup>6</sup>, Member, IEEE

**Abstract**—Very recent studies showed that the area spectral efficiency (ASE) of downlink cellular networks will continuously decrease and finally crash to zero as the base station (BS) density increases toward infinity if the absolute height difference between BS antenna and user equipment antenna is larger than zero. Such a phenomenon is referred to as the ASE crash. We revisit this issue by considering optimizing the BS antenna downtilt in cellular networks. It is common to adjust antenna pattern to tune the direction of the vertical beamforming and thus increasing received signal power and/or reducing inter-cell interference power to improve network performance. This paper focuses on investigating the relationship between the BS antenna downtilt and the downlink network performance in terms of the coverage probability and the ASE. Our results reveal an interesting find that there exists an optimal antenna downtilt to achieve the maximum coverage probability for each BS density. Numerically solvable expressions are derived for such optimal antenna downtilt, which is a function of the BS density. Our numerical results show that after applying the optimal antenna downtilt, the network performance can be significantly improved, and hence the ASE crash can be delayed by nearly one order of magnitude in terms of the BS density. Our results also give guidance on setting the optimum downtilt angle to maximize network performance given a fixed BS density.

**Index Terms**—Antenna downtilt, small cell network (SCN), coverage probability, area spectral efficiency (ASE), stochastic geometry.

## I. INTRODUCTION

IT HAS been widely acknowledged that wireless networks continue to face significant challenges and

opportunities [1]. In the first decade of 2000, network densification continued to underpin the capacity increases in the 3rd Generation Partnership Project (3GPP) 4th-generation (4G) Long Term Evolution (LTE) networks, and is expected to remain as one of the main forces to drive the 5th-generation (5G) networks onward [2]. Various emerging technologies have been developed in this context, such as small cell networks (SCNs), cognitive radio, massive MIMO, etc [3]. In particular, in the past few years, a few noteworthy studies have been carried out to revisit the performance analyses for cellular networks under more practical propagation models. In [4], the authors considered a multi-slope piece-wise path loss function, while in [5], the authors investigated line-of-sight (LoS) and non-line-of-sight (NLoS) transmission as a probabilistic event for a millimeter wave communication scenario. The most important finding in these two works is that the per-BS coverage probability performance starts to decrease when the base station (BS) density is sufficiently large. Fortunately, such a decrease of the coverage probability will not change the monotonic increase of the area spectral efficiency (ASE) as the BS density increases [4], [5]. However, in very recent works, the authors in [6]–[8] found that the ASE performance will continuously decrease toward zero with the network densification for SCNs when the absolute antenna height difference between a base station and a user equipment (UE) is larger than zero, which is referred to as the ASE Crash [6]–[8].

Having a closer look at the problem, we realize that in a three-dimensional (3D) channel model, the antenna patterns may increase the received signal and at the same time reduce inter-cell interference [9]. In particular, horizontal beamforming is a signal processing method that generates directional antenna beam patterns using multiple antennas at the transmitter. It is possible to steer the transmitted signal toward the desired direction and, at the same time, avoid receiving the unwanted signals from undesired directions [10]. The benefits of horizontal beamforming in cellular networks are well-understood and such technology has already been adopted in the LTE networks, e.g., the macro BSs. However, vertical beamforming (based on an antenna downtilt) receives much less attention. Recent studies have made some initial efforts that shed new light on adjusting antenna downtilt to improve the performance of cellular networks [11]–[13], but most of these studies were solely based on computer simulations.

In this paper, we investigate the impact of the antenna pattern and downtilt on the performance of the downlink (DL)

Manuscript received September 5, 2018; revised January 18, 2019; accepted January 24, 2019. Date of publication February 11, 2019; date of current version March 11, 2019. The associate editor coordinating the review of this paper and approving it for publication was R. Dinis. (Corresponding author: De-Gan Zhang.)

J. Yang is with the School of Electrical and Data Engineering, University of Technology Sydney, Sydney, NSW 2007, Australia (e-mail: junnan.yang@student.uts.edu.au).

M. Ding is with Data61, CSIRO, Sydney, NSW 2015, Australia (e-mail: ming.ding@data61.csiro.au).

G. Mao is with the School of Electrical and Data Engineering, University of Technology Sydney, Sydney, NSW 2007, Australia (e-mail: g.mao@ieee.org).

Z. Lin is with the School of Electrical and Information Engineering, The University of Sydney, Sydney, NSW 2006, Australia (e-mail: zihuai.lin@sydney.edu.au).

D.-G. Zhang is with the Key Lab of Computer Vision and System, Ministry of Education, Tianjin University of Technology, Tianjin 300384, China (e-mail: gandegande@126.com).

T. H. Luan is with the School of Cyber Engineering, Xidian University, Xi'an 710126, China (e-mail: tom.luan@xidian.edu.cn).

Color versions of one or more of the figures in this paper are available online at <http://ieeexplore.ieee.org>.

Digital Object Identifier 10.1109/TWC.2019.2897296

cellular networks, in terms of the coverage probability and the area spectral efficiency. We also derive the analytical expressions for the optimal antenna downtilt that can achieve the best coverage probability of the network given a certain BS density.

Compared with the existing works, the main contributions of this paper are:

- Based on the 3D antenna pattern model which includes horizontal and vertical antenna patterns, possibly with sectorization. We analytically investigate the relationship between the antenna downtilt and the cellular network performance in terms of the coverage probability and the ASE. Our results reveal an interesting finding that there exists a unique optimal antenna downtilt that strikes a balance between increasing the received signal power and reducing the interference power to achieve the maximum coverage probability for a certain BS density.
- We study and analyze the optimal antenna downtilt for a certain BS density with considering the 3D antenna pattern model which includes horizontal and vertical antenna patterns. As a consequence, we derive numerically solvable expressions for the optimal antenna downtilt for a certain BS density, which including three components, namely the LoS links, the NLoS links, and the noise, contributing to the optimal antenna downtilt.
- Our theoretical and numerical results demonstrate that the performance of the cellular network can be improved significantly using the optimal antenna downtilt. In particular, applying the optimal antenna downtilt can delay the ASE crash by nearly one order of magnitude in terms of the base station density. Using the derived expressions and the simulation results, network operators optimally select determine the antenna downtilt of BSs to maximize the system throughput for a given the base station density.

The rest of this paper is structured as follows. Section II provides a brief review of the related work. Section III describes the system model of the 3D cellular network. Section IV presents our theoretical results on the coverage probability, the optimal antenna downtilt and the simplified results for 3GPP special cases. Numerical results are discussed in Section V, with remarks shedding new light on the relevance of our results in guiding the network deployment. Finally, conclusions are drawn in Section VI.

## II. RELATED WORK

Stochastic geometry has been widely used to analyze the network performance [14], [15]. Andrews *et al.* [14] and Novlan *et al.* [15] conducted network performance analyses for the downlink (DL) and the uplink (UL) of SCNs, in which user equipment (UEs) and/or base stations (BSs) were assumed to be randomly deployed according to a homogeneous Poisson point process (HPPP). Furthermore, a stochastic model of the 3D environment was used to evaluate the network performance [6], [16]–[18]. Ding and López-Pérez [6] presented a new finding that if the absolute height difference between BS antenna and UE antenna is larger than zero, then the ASE performance will continuously decrease toward zero with the network densification for SCNs. In [18], the authors investigated

the performance of the small cell networks with considering the anisotropic path loss fading in wireless channels.

The benefits of horizontal beamforming in cellular networks are well-understood. The authors in [19] considered the sectorized antennas in the analysis and investigated the performance of the network. The authors in [5] also incorporated directional beamforming by modeling the beamforming gains as marks of the base station PPPs. On the other hand, many researchers have realized that a practical antenna can target its antenna beam towards a given direction via downtilt in the vertical domain, which may be exploited to improve the network performance [9], [20]–[23]. For example, the authors in [9] found via an empirical study that the antenna downtilt could bring a significant improvement to the cellular network capacity. In [20], the authors showed that vertical beamforming could increase the SIR by about 5-10 dB for a set of UE locations. Seifi *et al.* [21] investigated the performance impact of using antenna downtilt in traditional hexagonal 3D cellular networks. In [22], the author first time investigate the impact of the antenna downtilt on the coverage probability and shows the optimal antenna downtilt for two specific BS densities by simulations. In [23], the author first investigated the joint beamforming and tilt angle optimization which maximizes the total energy efficiency in downlink transmission multi-cell cellular network. However, most of the works investigated the impact of the antenna downtilt using field trials or simulations. To the best of our knowledge, none of the existing works have analytically studied the impact of the antenna downtilt of BSs on the cellular network performance and the empirical approach in these studies limits extension of their finding to more general scenarios.

In this work, we will investigate the impact of the antenna pattern and downtilt on the performance of the downlink (DL) cellular networks with a focus on analytically studying for the optimal antenna downtilt to achieve the best coverage probability of the network for a given and fixed BS density. It is important to note that our study can also be applied to drone networks flying at a certain altitude [24].

## III. SYSTEM MODEL

In this section, we will first explain the scenario of the 3D random cellular network. Then, we will present the antenna patterns and user association scheme considered in this work.

### A. Scenario Description

We consider a 3D random cellular network with downlink (DL) transmissions, where BSs are deployed on a plane according to an HPPP  $\Phi_b$  of intensity  $\lambda_B$  BSs/km<sup>2</sup>. UEs are also Poissonly distributed in the considered area with an intensity of  $\lambda_{UE}$  UEs/km<sup>2</sup>. Fig.1 shows an illustration of the considered network. In this model, BSs transmit at a power  $P_B$ , a UE can reliably communicate with a BS only when its downlink signal-to-interference-plus-noise ratio (SINR) is greater than  $\gamma$ . For each base station, we consider there are  $S$  sectors. We only consider one antenna in each sector and only the main lobe beamforming gain is considered, the beamforming includes the the horizontal and vertical antenna beamforming gain. In the same BS tower, the horizontal angle between

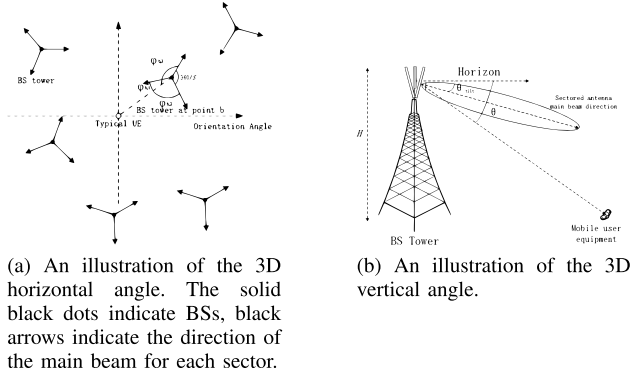


Fig. 1. An illustration of the network with randomly deployed BSs (For example,  $S = 3$ ).

the main beams of two adjacent sectors is set to  $\frac{360}{S}$  degrees. The orientations of the sectors are randomly and uniformly distributed in  $[0, 2\pi)$ . For example, for LTE macrocell BSs,  $S = 3$  and the horizontal angle between two adjacent sectors in the same BS tower is 120 degrees. Each sector has the vertical antenna pattern, we denote the horizontal direction as 0 degree. Hence, the vertical antenna downtilt angle and the angle from the BS antenna to the UE antenna by  $\theta_{tilt}$  and  $\theta$ , respectively, as shown in Fig.1b.

Without loss of generality, we conduct analysis and simulation on a typical mobile user located at the origin, similar to [5], [25], and [26]. Note that  $\lambda_{UE}$  is assumed to be sufficiently larger than  $\lambda_B$  so that each BS has at least one associated UE in its coverage [14], [27], [28]. The two-dimensional (2D) distance between an arbitrary BS and an arbitrary UE is denoted by  $r$ . Moreover, the absolute antenna height difference between a BS and a UE is denoted by  $L$ . Note that the value of  $L$  is in the order of several meters. Hence, the 3D distance  $w$  between a BS and a UE can be expressed as

$$w = \sqrt{r^2 + L^2}, \quad (1)$$

where  $L = H - h$  and  $H$  is the antenna height of BS and  $h$  is the antenna height of UE. Intuitively, the antenna height of BS should decrease as the network becomes dense, however, there is no consensus on how  $H$  should decrease with an increase in  $\lambda_B$ . In this work, we assume that  $H$ , and thus  $L$ , are constants. For the current 4G networks, parameter  $L$  is around 8.5m because the picocell BS antenna height and the UE antenna height are assumed to be 10m and 1.5m, respectively [11].

### B. Path Loss Model

The path loss function  $\zeta(w)$  is segmented into  $N$  pieces with each piece denoted by  $\zeta_n(w)$  [29]. Besides,  $\zeta_n^L(w)$ ,  $\zeta_n^{NL}(w)$  and  $\Pr_n^L(w)$  are the  $n$ -th piece of the path loss function for the LoS transmission, the  $n$ -th piece of the path loss function for the NLoS transmission, and the  $n$ -th piece of the LoS probability

function, respectively. It can be written as

$$\zeta(w) = \begin{cases} \zeta_1(w) = \begin{cases} \zeta_1^L(w), & \text{with probability } \Pr_1^L(w) \\ \zeta_1^{NL}(w), & \text{with probability } (1 - \Pr_1^L(w)) \end{cases} \\ \zeta_2(w) = \begin{cases} \zeta_2^L(w), & \text{with probability } \Pr_2^L(w) \\ \zeta_2^{NL}(w), & \text{with probability } (1 - \Pr_2^L(w)) \end{cases} \\ \vdots \\ \zeta_n(w) = \begin{cases} \zeta_n^L(w), & \text{with probability } \Pr_n^L(w) \\ \zeta_n^{NL}(w), & \text{with probability } (1 - \Pr_n^L(w)). \end{cases} \end{cases} \quad (2)$$

Each piece  $\zeta_n(w)$ ,  $n \in \{1, 2, \dots, N\}$  is modeled as

$$\zeta_n(w) = \begin{cases} \zeta_n^L(w) = A^L w^{-\alpha_n^L}, & \text{LoS Probability: } \Pr_n^L(w) \\ \zeta_n^{NL}(w) = A^{NL} w^{-\alpha_n^{NL}}, & \text{NLoS Probability: } 1 - \Pr_n^L(w), \end{cases} \quad (3)$$

where  $A^L$  and  $A^{NL}$  are the path losses at a reference distance  $w = 1$  for the LoS and the NLoS cases, respectively.  $\alpha_n^L$  and  $\alpha_n^{NL}$  are the path loss exponents for the LoS and the NLoS cases, respectively. In practice,  $A^L$ ,  $A^{NL}$ ,  $\alpha_n^L$  and  $\alpha_n^{NL}$  are constants obtainable from field tests and continuity constraints [30]. The LoS probability can be computed by the following piecewise function modeled as [7],

$$\Pr^L(w) = \begin{cases} \Pr_1^L(w), & L < w \leq d_1 \\ \Pr_2^L(w), & d_1 < w < d_2 \\ \vdots & \vdots \\ \Pr_n^L(w), & w > d_{n-1}, \end{cases} \quad (4)$$

which means the link from the typical UE to the typical BS has a LoS path or a NLoS path with probability  $\Pr^L(w)$  and  $1 - \Pr^L(w)$ , respectively,  $n \in \{1, 2, \dots, N\}$ .

### C. 3D Antenna Patterns

3D antenna patterns are introduced in this subsection. According to [2] and the 3GPP [11], UE antenna pattern is assumed to be isotropic and the 3D antenna gain of each sector antenna in the BS can be approximated in dBi as

$$G(\varphi_{b,i}, \theta_b, \theta_{tilt})^{\text{dBi}} = G_h(\varphi_{b,i}) + G_v(\theta_b, \theta_{tilt}) + G_m, \quad (5)$$

where  $G_h(\varphi_{b,i})$  and  $G_v(\theta_b, \theta_{tilt})$  are the normalized horizontal and vertical antenna gain from the  $i$ -th sector of the BS at point  $b$  to the typical UE in dBi, respectively.  $G_m$  is the maximum antenna gain. The 3D pattern is assumed to be fixed, i.e., no adaptive beamforming is employed. The parameter  $\varphi_{b,i}$  is the horizontal angle relative the main lobe beam pointing direction from the  $i$ -th ( $i \in 1, 2, 3, \dots, S$ ) sector of the BS at point  $b$  to the typical UE, i.e., horizontal departure angles for one BS-to-UE link. For the BS to UE link, there are  $S$  horizontal departure angles for the  $S$  sectors' antennas, we sort such angles in an ascending order and denote them as  $\varphi_{b,1} \leq \dots \leq \varphi_{b,S}$ , where  $b$  is point in the map which represent the BS location. An example is shown in Fig.1a. As we denote the

horizontal direction as 0 degree,  $\theta_{tilt}$  is the downtilt angle of the BS antennas, and  $0 \leq \theta_{tilt} \leq 90$  degrees is the negative elevation angle relative the horizontal plane (i.e.,  $\theta_{tilt} = 0$  is along the horizontal plane, and  $\theta_{tilt} \geq 0$  is downwards).  $\theta_b = \arctan\left(\frac{L}{r_b}\right)$  is the angle between the horizontal direction and the direction from the BS at point  $b$  to the typical UE. Parameter  $r_b$  is the distance from the BS at point  $b$  to the typical UE.

#### D. User Association and Performance Metrics

In this paper, we assume a practical user association strategy (UAS) that each UE connects to the sector of the BS with the strongest average received power strength  $P^*$  [5], [7] which can be written as

$$P^* = \max_{\Phi_b} \{P_B G(\varphi_{b,i}, \theta_b, \theta_{tilt}) \zeta_b(d_b)\} \quad (6)$$

where  $G(\varphi_{b,i}, \theta_b, \theta_{tilt}) = 10^{\frac{1}{10}G(\varphi_{b,i}, \theta_b, \theta_{tilt})^{dB}}$ ,  $d_b$  is the distance from the BS at point  $b$  to the typical UE.  $P_B$  and  $\zeta_b(d_b)$  are the transmission power of BS and the path loss from the BS at the point  $b$  to the typical UE, respectively.

Based on the above definitions, when the user associates with the sector of the macrocell BS at point  $\bar{X}$ , we define the coverage probability as a probability that a receiver's signal-to-interference-plus-noise ratio (SINR) is above a pre-designated threshold  $\gamma$ :

$$p^{\text{cov}}(\lambda_B, \gamma) = \Pr[\text{SINR} > \gamma], \quad (7)$$

where the SINR is calculated as

$$\text{SINR} = \frac{P_B G(\varphi_{\bar{b},1}, \theta_b, \theta_{tilt}) \zeta_{\bar{b}}(r) g}{I_{\text{agg}} + N_0}, \quad (8)$$

where  $g$  is the channel gain of Rayleigh fading, which is modeled as an exponential random variable (RV) with a mean of one. Parameter  $r$  is the distance from the associated BS at point  $\bar{b}$  to the typical UE. Parameter  $N_0$  is the additive white Gaussian noise (AWGN) power at each UE. Parameter  $I_{\text{agg}}$  is the cumulative interference given by

$$I_{\text{agg}} = \sum_{i=2}^S P_B G(\varphi_{\bar{b},i}, \theta_b, \theta_{tilt}) \zeta_{\bar{b}}(r) g_{\bar{b}} + \sum_{b \in \Phi_b/\bar{b}} \sum_{i=1}^S P_B G(\varphi_{b,i}, \theta_b, \theta_{tilt}) \zeta_b(d_b) g_b. \quad (9)$$

where  $d_b$  is the distance from the BS at point  $b$  to the typical UE. The symbol  $\zeta_b(d_b)$  is the path loss function from the BS at point  $b$  to the typical UE. The first term of Eq.(9) represents the intra-cell inter-sector interference while the second represents the inter-cell interference.

Similar to [7] and [28], the area spectral efficiency in bps/Hz/km<sup>2</sup> can be formulated as

$$A^{\text{ASE}}(\lambda_B, \gamma_0) = \lambda_B \int_{\gamma_0}^{\infty} \log_2(1+x) f_X(\lambda_B, \gamma_0) dx, \quad (10)$$

where  $\gamma_0$  is the minimum working SINR for the considered network, and  $f_X(\lambda_B, \gamma_0)$  is the probability density function (PDF) of the SINR observed at the typical receiver for a particular value of  $\lambda_B$ .

## IV. MAIN RESULTS

Using the 3D model and the stochastic geometry theory, we study the performance of the cellular network and derive the optimal antenna downtilt for each certain base station density in this section. Without any loss of generality, we assume that the mobile user under consideration is located at the origin.

### A. The Coverage Probability

Based on the path loss model in Eq.(2) and the adopted UAS, our results of  $p^{\text{cov}}(\lambda_B, \gamma)$  can be summarized in Theorem 1.

*Theorem 1: Considering the path loss model in Eq.(2) and the presented UAS, the probability of coverage  $p^{\text{cov}}(\lambda_B, \gamma)$  can be derived as*

$$p^{\text{cov}}(\lambda_B, \gamma) = \sum_{n=1}^N (T_n^L + T_n^{NL}) \quad (11)$$

where

$$T_n^L = \int_0^{\frac{\pi}{S}} \int_{\sqrt{d_{n-1}^2 - L^2}}^{\sqrt{d_n^2 - L^2}} \times \Pr\left[\frac{P_B G(\varphi_{\bar{b},1}, \theta_b, \theta_{tilt}) \zeta_{\bar{b}}^L(w) g_{\bar{b}}}{I_{\text{agg}} + N_0} > \gamma \mid w, \varphi_{\bar{b},1}\right] \times f_{R,n}^L(r) f(\varphi) dr d\varphi \quad (12)$$

which represent the signal is in the  $n$ -th piece of path loss function for the LoS transmission,

$$T_n^{NL} = \int_0^{\frac{\pi}{S}} \int_{\sqrt{d_{n-1}^2 - L^2}}^{\sqrt{d_n^2 - L^2}} \times \Pr\left[\frac{P_B G(\varphi_{\bar{b},1}, \theta_b, \theta_{tilt}) \zeta_{\bar{b}}^{NL}(w) g_{\bar{b}}}{I_{\text{agg}} + N_0} > \gamma \mid w, \varphi_{\bar{b},1}\right] \times f_{R,n}^{NL}(r) f(\varphi) dr d\varphi \quad (13)$$

which represent the signal is in the  $n$ -th piece of path loss function for the NLoS transmission.  $I_{\text{agg}}$  is the aggregation interference from the LoS path and NLoS path.  $f(\varphi)$  is the distribution of the smallest horizontal angle from the signal BS to the typical UE. Based on the assumptions in the system model, the angle  $\varphi$  is uniformly distributed in  $[0, \frac{\pi}{S}]$ , so  $f(\varphi) = \frac{S}{\pi}$  when  $0 < \varphi < \frac{\pi}{S}$ . Where  $f_{R,n}^L(r)$  and  $f_{R,n}^{NL}(r)$  are the distance distribution of the  $n$ -piece signal link when the link is LoS and NLoS, which can be written as

$$f_{R,n}^L(r) = \exp\left(-\int_0^{r^2} \Pr_n^L(u) 2\pi u \lambda_B du\right) \times \exp\left(-\int_0^{r^2} (1 - \Pr_n^L(u)) 2\pi u \lambda_B du\right) \times \exp\left(-\int_0^r \Pr_n^L(u) 2\pi u \lambda_B du\right) \times \Pr_n^L(u) 2\pi u \lambda_B, \quad (14)$$

$$f_{R,n}^{NL}(r) = \exp\left(-\int_0^{r^4} \Pr_n^L(u) 2\pi u \lambda_B du\right) \times \exp\left(-\int_0^{r^4} (1 - \Pr_n^L(u)) 2\pi u \lambda_B du\right)$$

$$\begin{aligned} & \times \exp\left(-\int_0^r (1 - \Pr_n^L(u)) 2\pi u \lambda_B du\right) \\ & \times (1 - \Pr_n^L(u)) 2\pi u \lambda_B \end{aligned} \quad (15)$$

where  $r_{\{1,2,3,4\}}$  are given implicitly by the following equations as

$$r_1^2 = \left(\frac{G(\varphi_{\bar{b},1}, \theta_{\bar{b}}, \theta_{\text{tilt}}) A_L}{G(\varphi_{b_1,1}, \theta_{b_1}, \theta_{\text{tilt}}) A_{NL}}\right)^{-\frac{2}{\alpha_{NL}}} (r^2 + L^2)^{\frac{\alpha_L}{\alpha_{NL}}} \quad (16)$$

and

$$r_2^2 = \left(\frac{G(\varphi_{\bar{b},1}, \theta_{\bar{b}}, \theta_{\text{tilt}})}{G(\varphi_{b_2,1}, \theta_{b_2}, \theta_{\text{tilt}})}\right)^{-\frac{2}{\alpha_L}} (r^2 + L^2) \quad (17)$$

and

$$r_3^2 = \left(\frac{G(\varphi_{\bar{b},1}, \theta_{\bar{b}}, \theta_{\text{tilt}})}{G(\varphi_{b_3,1}, \theta_{b_3}, \theta_{\text{tilt}})}\right)^{-\frac{2}{\alpha_{NL}}} (r^2 + L^2) \quad (18)$$

and

$$r_4^2 = \left(\frac{G(\varphi_{\bar{b},1}, \theta_{\bar{b}}, \theta_{\text{tilt}}) A_{NL}}{G(\varphi_{b_4,1}, \theta_{b_4}, \theta_{\text{tilt}}) A_L}\right)^{-\frac{2}{\alpha_L}} (r^2 + L^2)^{\frac{\alpha_{NL}}{\alpha_L}}, \quad (19)$$

$\Pr\left[\frac{P_B G(\varphi_{\bar{b},1}, \theta_{\bar{b}}, \theta_{\text{tilt}}) \zeta_b^L(w) g_{\bar{b}}}{I_r + N_0} > \gamma \mid w, \varphi_{\bar{b},1}\right]$   
 $\Pr\left[\frac{P_B G(\varphi_{\bar{b},1}, \theta_{\bar{b}}, \theta_{\text{tilt}}) \zeta_b^{NL}(w) g_{\bar{b}}}{I_r + N_0} > \gamma \mid w, \varphi_{\bar{b},1}\right]$  can be respectively computed by

$$\begin{aligned} & \Pr\left[\frac{P_B G(\varphi_{\bar{b},1}, \theta_{\bar{b}}, \theta_{\text{tilt}}) \zeta_b^L(w) g_{\bar{b}}}{I_r + N_0} > \gamma \mid w, \varphi_{\bar{b},1}\right] \\ & = \exp\left(-\frac{\gamma N_0}{P_B G(\varphi_{\bar{b},1}, \theta_{\bar{b}}, \theta_{\text{tilt}}) A^L (r^2 + L^2)^{-\frac{\alpha_L}{2}}}\right) \\ & \quad \times \mathcal{L}_{I_{\text{agg}}}\left(\frac{\gamma}{P_B G(\varphi_{\bar{b},1}, \theta_{\bar{b}}, \theta_{\text{tilt}}) A^L (r^2 + L^2)^{-\frac{\alpha_L}{2}}}\right) \end{aligned} \quad (20)$$

and

$$\begin{aligned} & \Pr\left[\frac{P_B G(\varphi_{\bar{b},1}, \theta_{\bar{b}}, \theta_{\text{tilt}}) \zeta_b^{NL}(w) g_{\bar{b}}}{I_r + N_0} > \gamma \mid w, \varphi_{\bar{b},1}\right] \\ & = \exp\left(-\frac{\gamma N_0}{P_B G(\varphi_{\bar{b},1}, \theta_{\bar{b}}, \theta_{\text{tilt}}) A^{NL} (r^2 + L^2)^{-\frac{\alpha_{NL}}{2}}}\right) \\ & \quad \times \mathcal{L}_{I_{\text{agg}}}\left(\frac{\gamma}{P_B G(\varphi_{\bar{b},1}, \theta_{\bar{b}}, \theta_{\text{tilt}}) A^{NL} (r^2 + L^2)^{-\frac{\alpha_{NL}}{2}}}\right). \end{aligned} \quad (21)$$

where  $\mathcal{L}_{I_{\text{agg}}}\left(\frac{\gamma}{P_B G(\varphi_{\bar{b},1}, \theta_{\bar{b}}, \theta_{\text{tilt}}) A^L w^{-\alpha_L}}\right)$  and  $\mathcal{L}_{I_{\text{agg}}}\left(\frac{\gamma}{P_B G(\varphi_{\bar{b},1}, \theta_{\bar{b}}, \theta_{\text{tilt}}) A^{NL} w^{-\alpha_{NL}}}\right)$  are the Laplace transform of  $I_{\text{agg}}$  evaluated at  $s$  and  $I_{\text{agg}}$  is the aggregation interference at the typical UE.

*Proof:* See Appendix A.  $\blacksquare$

## B. The Optimal Antenna Downtilt

In order to get the optimal antenna downtilt to maximize the coverage probability, we take the derivative of the coverage probability and find the optimal point for each BS density. In this subsection, we first present Lemma 2 to show that there always exists a unique solution of the optimal antenna downtilt, and then we present the solution of the optimal antenna downtilt for a given BS density.

*Lemma 2:* For a typical UE, the coverage probability is a function of the antenna downtilt and there is a unique solution of the antenna downtilt to achieve the maximum coverage probability for a certain BS density.

*Proof:* The coverage probability can be written as follows,

$$\begin{aligned} & p^{\text{cov}}(\lambda_B, \gamma) \\ & = \int_0^{\frac{\pi}{8}} \int_0^\infty \Pr\left[\frac{P_B G(\varphi_{\bar{b},1}, \theta_b, \theta_{\text{tilt}}) \zeta(r) g}{I_{\text{agg}} + N_0} > \gamma \mid r\right] \\ & \quad \times f_R(r) f(\varphi) dr d\varphi \\ & = \int_0^{\frac{\pi}{8}} \int_0^\infty \Pr\left[g > \frac{\gamma (I_{\text{agg}} + N_0)}{P_B G(\varphi_{\bar{b},1}, \theta_b, \theta_{\text{tilt}}) \zeta(r)} \mid r\right] \\ & \quad \times f_R(r) f(\varphi) dr d\varphi \\ & = \int_0^\infty \mathbb{E}_{\text{signal}, I} \left[ \exp\left(-\frac{\gamma (I_{\text{agg}} + N_0)}{P_B G(\varphi_{\bar{b},1}, \theta_r, \theta_{\text{tilt}}) \zeta(r)}\right) \mid r \right] \\ & \quad \times f_R(r) dr \end{aligned} \quad (22)$$

where ‘signal’ means the average signal power for a typical UE,  $\zeta(r)$  is the path loss function.

From this equation, we can see that as long as the average SINR has one and only one maximum value, then the coverage probability also has one and only one maximum value. For a typical UE, the signal and cumulative interference expressions have been shown in Eq.(6) and Eq.(9), both the signal and interference power change with  $G(\varphi_{b,i}, \theta_b, \theta_{\text{tilt}})$ . In particular,  $G(\varphi_{b,i}, \theta_b, \theta_{\text{tilt}})$  changes with the antenna downtilt and it achieves the maximum value when  $\theta_{\text{tilt}} = \theta_b = \arctan\left(\frac{L}{d}\right)$ , where  $L$  is the height difference and  $d$  is the distance from transmitter to the receiver. Based on the antenna pattern model, both the signal power and the aggregate interference power are increasing as the antenna downtilt grows from 0 degree and then decreasing as the antenna gradually looks downward. As the antenna downtilt increases, the aggregate interference will hit the maximum level earlier than the signal power because the average distance from the interfering BSs to the typical UE is larger than the distance from the associated BS to the typical UE. Then, the average signal continually increases and the interference decreases. So, the SINR expression will increase at this stage. When  $\theta_{\text{tilt}} > \arctan\left(\frac{L}{r}\right)$ , where  $r$  is the distance from the typical BS to the typical UE, both the signal power and the aggregate interference power are decreasing. During this stage, the decreasing rate of the signal power is larger than the decreasing rate of the interference power with respect to the antenna downtilt as the average distance from the associated BS to the typical UE is smaller than the distance from the interfering BSs to the typical UE, and hence the change of the antenna downtilt angle has a larger impact on the former case than that on the latter one, according to the antenna pattern model addressed in Subsection III-C.

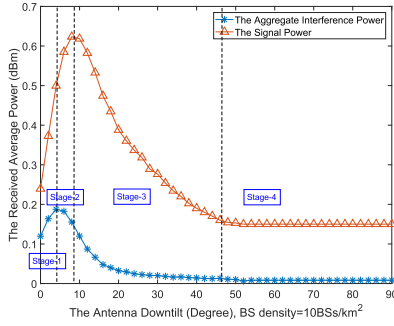


Fig. 2. The average signal and cumulative interference power with antenna downtilt and a BS density of 10BSs/km<sup>2</sup>.

There are two possible cases for the SINR expression: 1) It increases first and then decreases; 2) It monotonically decreases. In both cases, there exists a solution of antenna downtilt to achieve the maximum coverage probability for a certain BS density during this stage. In addition, both the interference and the signal power expressions are all concave functions with respect to the antenna downtilt when  $\theta_{tilt} > \arctan\left(\frac{L}{r}\right)$  so that the average SINR function is a concave function. Hence there only exists one optimal point, which concludes our proof. ■

It is difficult to have a more concrete proof, so we using the toy example to explain this question based on the SINR statistics on average.

*Remark 3:* As a toy example, the signal power and the aggregate interference power have been plotted in Fig. 2 assuming the LTE macrocell BS model with a BS density of 10 BSs/km<sup>2</sup>.

As the aggregate interference hits its maximum earlier than the signal power, there are four stages of the functions of the signal power and the aggregate interference power as the antenna downtilt increases from 0 to 90 degrees. In stage 1, both the signal power and the aggregate interference power will initially increase as the antenna downtilt grows from zero. The increasing rate of the signal power is larger than the increasing rate of the aggregate interference power with respect to the antenna downtilt. Hence, the average SINR function will increase during stage 1. In stage 2, the aggregate interference power becomes a monotonically decreasing function and the signal power will continue increasing with respect to the antenna downtilt. Hence, the average SINR function will continue increasing in stage 2. In stage 3, both the signal power and the aggregate interference power are decreasing. During this stage, the decreasing rate of the signal power is larger than the decreasing rate of the interference power with respect to the antenna downtilt. There are two possible cases for the SINR function: 1) It increases first and then decreases; 2) It monotonically decreases. In both cases, there exists a solution of antenna downtilt in stage 2 or 3 to achieve the maximum coverage probability for a certain BS density. In stage 4, both the interference and the signal power are constants. Hence, the average SINR function becomes a constant independent of the antenna downtilt. To sum up, there exists a unique solution of antenna downtilt in stage 2 or 3 to achieve the maximum coverage probability for a certain BS density.

In the following, we will present such a unique and optimal antenna downtilt with respect to the BS density, which is summarized as Theorem 4.

*Theorem 4:* For a certain BS density  $\lambda_B$ , the optimal antenna downtilt can be found by the following equation:

$$\theta_{tilt} = \arg_{\theta_{tilt}} \left\{ dP_c^L(\theta_{tilt}) + dP_c^{NL}(\theta_{tilt}) + dP_c^{Noise}(\theta_{tilt}) = 0 \right\} \quad (23)$$

where

$$\begin{aligned} dP_c^L(\theta_{tilt}) &= -2\pi\lambda_B \sum_{n=1}^N \int_{\sqrt{d_n^2-L^2}}^{\sqrt{d_n^2-L^2}} \int_r^\infty (\text{Pr}_n^L(u)) \gamma \times \left( \frac{u^2 + L^2}{r^2 + L^2} \right)^{\frac{\alpha L}{2}} \\ &\times \left[ \frac{u \sum_{n=1}^S \frac{\partial G(\varphi_{b,n}, \theta_u, \theta_{tilt})}{\partial \theta_{tilt}} G(\varphi_{b,1}, \theta_r, \theta_{tilt})}{\left( \gamma a + G(\varphi_{b,1}, \theta_r, \theta_{tilt}) \left( \frac{u^2 + L^2}{r^2 + L^2} \right)^{\frac{\alpha L}{2}} \right)^2} \right. \\ &\left. - \frac{\frac{\partial G(\varphi_{b,1}, \theta_r, \theta_{tilt})}{\partial \theta_{tilt}} \sum_{n=1}^S G(\varphi_{b,n}, \theta_u, \theta_{tilt})}{\left( \gamma a + G(\varphi_{b,1}, \theta_r, \theta_{tilt}) \left( \frac{u^2 + L^2}{r^2 + L^2} \right)^{\frac{\alpha L}{2}} \right)^2} \right] \\ &\times f_{R,n}^L(r) dudr - 2\pi\lambda_B \sum_{n=1}^N \int_{\sqrt{d_n^2-L^2}}^{\sqrt{d_n^2-L^2}} \\ &\times \int_r^\infty (\text{Pr}_n^L(u)) A^L A^{NL} \gamma \times \left( \frac{u^2 + L^2}{(r^2 + L^2)^{\frac{\alpha L}{2}}} \right)^{\frac{\alpha L}{2}} \\ &\times \left[ \frac{u \sum_{n=1}^S \frac{\partial G(\varphi_{b,n}, \theta_u, \theta_{tilt})}{\partial \theta_{tilt}} G(\varphi_{b,1}, \theta_r, \theta_{tilt})}{\left( \gamma A^L a + \frac{G(\varphi_{b,1}, \theta_r, \theta_{tilt}) A^{NL} (u^2 + L^2)^{\frac{\alpha L}{2}}}{(r^2 + L^2)^{\frac{\alpha NL}{2}}} \right)^2} \right. \\ &\left. - \frac{\frac{\partial G(\varphi_{b,1}, \theta_r, \theta_{tilt})}{\partial \theta_{tilt}} \sum_{n=1}^S G(\varphi_{b,n}, \theta_u, \theta_{tilt})}{\left( \gamma A^L a + \frac{G(\varphi_{b,1}, \theta_r, \theta_{tilt}) A^{NL} (u^2 + L^2)^{\frac{\alpha L}{2}}}{(r^2 + L^2)^{\frac{\alpha NL}{2}}} \right)^2} \right] \\ &\times f_{R,n}^{NL}(r) dudr, \quad (24) \\ dP_c^{NL}(\theta_{tilt}) &= -2\pi\lambda_B \sum_{n=1}^N \int_{\sqrt{d_n^2-L^2}}^{\sqrt{d_n^2-L^2}} (1 - \text{Pr}_n^L(u)) \\ &\times A^L A^{NL} \gamma \frac{(u^2 + L^2)^{\frac{\alpha NL}{2}}}{(r^2 + L^2)^{\frac{\alpha L}{2}}} \\ &\times \left[ \frac{u \sum_{n=1}^S \frac{\partial G(\varphi_{b,n}, \theta_u, \theta_{tilt})}{\partial \theta_{tilt}} G(\varphi_{b,1}, \theta_r, \theta_{tilt})}{\left( \gamma A^{NL} a + \frac{G(\varphi_{b,1}, \theta_r, \theta_{tilt}) A^L (u^2 + L^2)^{\frac{\alpha NL}{2}}}{(r^2 + L^2)^{\frac{\alpha L}{2}}} \right)^2} \right. \end{aligned}$$

$$\begin{aligned}
 & \left. - \frac{\frac{\partial G(\varphi_{\bar{b},1}, \theta_r, \theta_{tilt})}{\partial \theta_{tilt}} \sum_{n=1}^S G(\varphi_{b,n}, \theta_u, \theta_{tilt})}{\left( \gamma A^{NL} a + \frac{G(\varphi_{\bar{b},1}, \theta_r, \theta_{tilt}) A^L (u^2 + L^2)^{\frac{\alpha_{NL}}{2}}}{(r^2 + L^2)^{\frac{\alpha_L}{2}}} \right)^2} \right] \\
 & \times f_{R,n}^L(r) dudr \\
 & - 2\pi \lambda_B \sum_{n=1}^N \int_{\sqrt{d_{n-1}^2 - L^2}}^{\sqrt{d_n^2 - L^2}} (1 - \text{Pr}_n^L(u)) \gamma \left( \frac{u^2 + L^2}{r^2 + L^2} \right)^{\frac{\alpha_{NL}}{2}} \\
 & \times \left[ \frac{u \sum_{n=1}^S \frac{\partial G(\varphi_{b,n}, \theta_u, \theta_{tilt})}{\partial \theta_{tilt}} G(\varphi_{\bar{b},1}, \theta_r, \theta_{tilt})}{\left( \gamma a + G(\varphi_{\bar{b},1}, \theta_r, \theta_{tilt}) \left( \frac{u^2 + L^2}{r^2 + L^2} \right)^{\frac{\alpha_{NL}}{2}} \right)^2} \right. \\
 & \left. - \frac{\frac{\partial G(\varphi_{\bar{b},1}, \theta_r, \theta_{tilt})}{\partial \theta_{tilt}} \sum_{n=1}^S G(\varphi_{b,n}, \theta_u, \theta_{tilt})}{\left( \gamma a + G(\varphi_{\bar{b},1}, \theta_r, \theta_{tilt}) \left( \frac{u^2 + L^2}{r^2 + L^2} \right)^{\frac{\alpha_{NL}}{2}} \right)^2} \right] \\
 & \times f_{R,n}^{NL}(r) dudr, \\
 & dP_c^{Noise}(\theta_{tilt}) \\
 & = \sum_{n=1}^N \int_{\sqrt{d_{n-1}^2 - L^2}}^{\sqrt{d_n^2 - L^2}} (r^2 + L^2)^{\frac{\alpha_L}{2}} \\
 & \times \frac{\gamma N_0 \frac{\partial G(\varphi_{\bar{b},1}, \theta_r, \theta_{tilt})}{\partial \theta_{tilt}}}{P_B G^2(\varphi_{\bar{b},1}, \theta_r, \theta_{tilt}) A^L} f_{R,n}^L(r) dr \\
 & + \sum_{n=1}^N \int_{\sqrt{d_{n-1}^2 - L^2}}^{\sqrt{d_n^2 - L^2}} (r^2 + L^2)^{\frac{\alpha_{NL}}{2}} \\
 & \times \frac{\gamma N_0 \frac{\partial G(\varphi_{\bar{b},1}, \theta_r, \theta_{tilt})}{\partial \theta_{tilt}}}{P_B G^2(\varphi_{\bar{b},1}, \theta_r, \theta_{tilt}) A^{NL}} f_{R,n}^{NL}(r) dr
 \end{aligned} \tag{25}$$

where  $a = \sum_{n=1}^S G(\varphi_{b,n}, \theta_u, \theta_{tilt})$ ,  $f_{R,n}^L(r)$  and  $f_{R,n}^{NL}(r)$  can be found in Theorem 1,  $\frac{\partial G(\varphi_{\bar{b},1}, \theta_r, \theta_{tilt})}{\partial \theta_{tilt}}$ ,  $\frac{\partial G(\varphi_{b,n}, \theta_u, \theta_{tilt})}{\partial \theta_{tilt}}$  are the derivatives for  $\theta_{tilt}$ .

*Proof:* See Appendix B. ■

From Theorem 4, we can draw the following insights:

- There are three components in Eq.(23) which contribute to the optimal antenna downtilt, include the LoS links and the NLoS links shown in Eq.(24) and Eq.(25) and the noise shown in Eq.(26), respectively.
- When the networks are sparse, the signal is mostly NLoS and the noise is the dominant factor. Therefore, the NLoS links and noise are the major ones that determine the optimal downtilt. As the BS density increases, most signals and some interference links transit from NLoS to LoS, and hence, all components in Eq.(23) should be taken into account. When the BS density is sufficiently large, almost all signals and the major interference links are LoS, and the noise is negligible compared to the signal or interference. Therefore, the LoS links become the major component that determines the optimal downtilt.

### C. Study of 3GPP Cases

1) *The Special Case of the Path Loss Functions:* As the main purpose of this work is to investigate the relationship between network performance and the antenna downtilt, we consider a simplified version of the aforementioned path loss model, that is a two-piece path loss model, and a linear LoS probability function defined by the 3GPP [31] as a special case in the numerical part. The path loss model can be written as

$$\zeta(w) = \begin{cases} A^L w^{-\alpha_L}, & \text{LoS Probability: } \text{Pr}^L(w) \\ A^{NL} w^{-\alpha_{NL}}, & \text{NLoS Probability: } 1 - \text{Pr}^L(w), \end{cases} \tag{27}$$

regarding realistic path loss models,

$$\text{Pr}^L(r) = \begin{cases} 1 - \frac{w}{d_1} & 0 < w \leq d_1 \\ 0 & w > d_1, \end{cases} \tag{28}$$

where  $d_1$  is the 3D cut-off distance of the LoS link for BS-to-UE links. The adopted linear LoS probability function is very useful because it can include other LoS probability functions as its special cases [7]. For the 3GPP special case, according to Theorem 1,  $p^{\text{cov}}(\lambda_B, \gamma)$  can then be computed by

$$p^{\text{cov}}(\lambda_B, \gamma) = T_1^L + T_1^{NL} + T_2^{NL}. \tag{29}$$

The results of the 3GPP special case can be obtained by plugging (27), (28) and  $n = 2$  into Theorem 1 and Theorem 3. We can obtain the coverage probability and the optimal antenna downtilt which is numerically solvable for the 3GPP case.

2) *The Special Case of the Antenna Pattern:* In this subsection, we will discuss the antenna pattern for both the LTE macrocell BS model and the LTE picocell BS model.

For the LTE macrocell BS model, we use 3 sectors BS tower and a 3D antenna pattern defined in [11] for each sector, where

$$G_h(\varphi_{b,i}) = -\min \left[ 12 \left( \frac{\varphi_{b,i}}{B_h} \right)^2, SLL_{az} \right], \tag{30}$$

and

$$G_v(\theta_b, \theta_{tilt}) = -\min \left[ 12 \left( \frac{\theta_b - \theta_{tilt}}{B_{v1}} \right)^2, SLL_{el} \right], \tag{31}$$

where  $B_h = 65$  degrees and  $B_{v1} = 10$  degrees are the horizontal and vertical half power beamwidth,  $SLL_{az} = 20\text{dB}$  and  $SLL_{el} = 20\text{dB}$  [32] are the side lobe levels (SLL) in the azimuth and elevation planes. The maximum antenna gain  $G_m = 14\text{dBi}$  from [31].

Using the Eq.(5), Eq.(30) and Eq.(31), we have

$$\frac{\partial G(\varphi_{\bar{b},1}, \theta_r, \theta_{tilt})}{\partial \theta_{tilt}} = \frac{2a_r}{b} (\theta_r - \theta_{tilt}) \exp \left[ -\frac{(\theta_r - \theta_{tilt})^2}{b} \right] \tag{32}$$

and

$$\frac{\partial G(\varphi_{b,n}, \theta_u, \theta_{tilt})}{\partial \theta_{tilt}} = \frac{2a_{u,i}}{b} (\theta_u - \theta_{tilt}) \exp \left[ -\frac{(\theta_u - \theta_{tilt})^2}{b} \right] \tag{33}$$

where  $\theta_r = \arctan\left(\frac{L}{r}\right)$ ,  $\theta_u = \arctan\left(\frac{L}{u}\right)$ ,  $a_r = 10^{\left[-1.2\left(\frac{\varphi_{b,1}}{B_h}\right)^2 + G_m\right]}$ ,  $a_{u,i} = 10^{\left[-1.2\left(\frac{\varphi_{u,i}}{B_h}\right)^2 + G_m\right]}$  are independent of  $\theta_{tilt}$ . Plugging Eq.(32) and Eq.(33) into Theorem 4, and considering the two-piece path loss model, we can obtain the optimal downtilt expressions for macrocell BSs.

Very similar to macrocell BSs, for the LTE picocell BS model, we consider a dipole antenna pattern to investigate the impact of the vertical downtilt. Note that such antenna pattern is more practical for the study of SCNs. The dipole antenna is omni-directional in horizontal direction, i.e.,  $G_h(\varphi_{b,i}) = 0\text{dB}$  [2], [33] and only one sector in one BS tower, i.e.,  $S = 1$ . With electrical downtilt [33], [34], the vertical pattern of the dipole antenna main lobe can be approximated as

$$G_v(\theta_b, \theta_{tilt}) = 10 \log_{10} |\cos^n(\theta_b - \theta_{tilt})|, \quad (34)$$

where  $n = 47.64$  for a 4-element half-wave dipole antenna.

## V. SIMULATION AND DISCUSSION

In this section, we investigate the network performance and use numerical results to establish the accuracy of our analysis. The 3GPP special cases studied in Section IV have been considered in this section. The analytical results are compared with Monte Carlo simulation results in terms of the coverage probability and the optimal antenna downtilt. According to the 3GPP standard [11], we adopt the following parameters:  $d_1 = 300\text{m}$ ,  $\alpha^L = 2$ ,  $\alpha^{NL} = 3.75$ ,  $A^L = 10^{-10.38}$ ,  $A^{NL} = 10^{-14.54}$ ,  $P_B = 46\text{dBm}$  for the LTE macrocell BSs while  $P_B = 24\text{dBm}$  for the LTE picocell BSs,  $P_N = -95\text{dBm}$  (including a noise figure of 9 dB at the receivers).

### A. Validation of Theorem 1 on the Coverage Probability

In this subsection, we present Monte Carlo simulation results to investigate the coverage probability and validate the analytical results in Theorem 1. In Fig.3, we plot the coverage probability for (i) the LTE macrocell BS model with two different BS densities and a BS height of 20m, and (ii) the LTE picocell BS model with two different BS heights and a BS density of 100 BSs/km<sup>2</sup>. The SINR threshold and the UE antenna height are set to  $\gamma = 0\text{dB}$  and 1.5m, respectively [11]. As can be seen from Fig.3, our analytical results, which are given by Theorem 1, match the simulation results very well, and we can draw the following observations:

- For a certain BS density, there exists an optimal antenna downtilt which can achieve the maximum coverage probability. Antenna downtilt has a significant impact on the coverage probability both in the LTE macrocell BS model and the LTE picocell BS model.
- The optimal antenna downtilt increases as the BS density increases because the denser the BS network, the more near-sighted the BS will look downward since the distance from the typical UE to its associated BS is generally shorter as the network becomes denser.

### B. Validation of Theorem 4 on the Optimal Antenna Downtilt

In this subsection, we validate the analytical results in Theorem 4 by providing Monte Carlo simulation results.

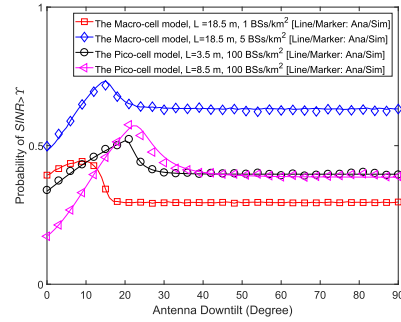


Fig. 3. Coverage probability vs. antenna downtilt of the LTE macrocell BS with  $\gamma = 0$  dB.

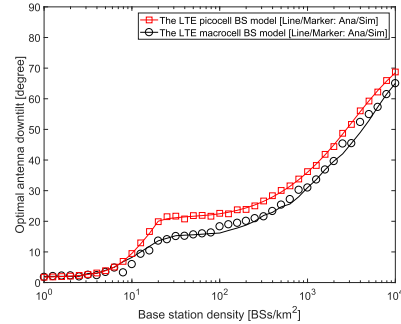
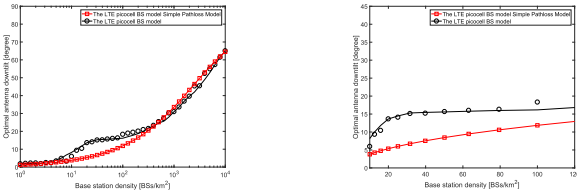


Fig. 4. Optimal antenna downtilt vs. base station density with  $\gamma = 0$  dB.

In Fig.4, we show the optimal downtilt of the LTE picocell model and the LTE macrocell model as the BS density increases with  $\gamma = 0\text{dB}$ . The antenna height difference  $L$  is set to 8.5m. As can be seen from Fig.4, our analytical results, given by Theorem 4, match the simulation results very well, which validates the accuracy of our analysis. Moreover, we can draw the following observations:

- Under the two different models, an optimal antenna downtilt can be found for any given base station density to obtain the highest coverage probability. The optimal antenna downtilt increases as the BS density increases.
- The optimal antenna downtilt shows a significant change of trend when the BS density is around  $10^{1.1}$  BSs/km<sup>2</sup>. This is because most signals and interference are NLoS when the networks are sparse (the BS density  $< 10$  BSs/km<sup>2</sup>) and these signals and the dominant interference begin to transit from NLoS to LoS when the BS density increases beyond  $10^{1.1}$  BSs/km<sup>2</sup>. Hence the increasing speed of the optimal antenna downtilt is slowing down since a strong LoS signal power supports a relatively small antenna downtilt.
- When considering the LTE macrocell BS model, the optimal antenna downtilt is smaller than the LTE picocell BS model because the antenna can look a bit farther to boost the signal power at the cell-edge area since the interference is less severe with the 3-sector directional antenna pattern.

In subsection V-A and V-B, we have verified the accuracy of our theoretical analysis. We can see that our theoretical analysis matches well with the numerical results. But in the 5G cellular network, it makes more sense to deploy the picocell BSs to serve the UEs which is an even denser network,



(a) Optimal Antenna downtilt vs. BS density of the LTE picocell model with adopted path loss model and the simple path loss model.

(b) Optimal Antenna downtilt vs. BS density 10 and 100 BSs/km<sup>2</sup> of the LTE picocell model with adopted path loss model and the simple path loss model.

Fig. 5. Optimal Antenna downtilt vs. BS density of the LTE picocell model with adopted path loss model and the simple path loss model.

i.e., the BS density is larger than 20 BSs/km<sup>2</sup>. Hence, we will focus on the LTE picocell model with the omni-directional antenna pattern to investigate the impact of the optimal antenna pattern on the network performance of dense networks in the following.

### C. The Optimal Antenna Downtilt With Simple Path Loss Model

In this subsection, we will show the optimal antenna downtilt with simple path loss model.

In Fig.5, we show the optimal downtilt of the LTE picocell model with the BS density increase with  $\gamma = 0\text{dB}$  and the optimal antenna downtilt with simple path loss model which is a single slope path loss model with  $\alpha = 3.75$ . As we can observe in Fig.5a and Fig.5b, we can draw the following observations:

- Between the BS density from 10 BSs/km<sup>2</sup> to 200 BSs/km<sup>2</sup>, the results with the LoS/NLoS first grow faster, then grow slower than that with a simple path loss model.
- From 35 BSs/km<sup>2</sup> and 100 BSs/km<sup>2</sup>, the optimal antenna downtilt remains almost the stable because some interference turn from the NLoS to LoS path, the optimal antenna downtilt need to reduce the sudden increase of the interference.

### D. The Performance Impact of BS Antenna Height on the Coverage Probability

In this subsection, we consider the omni-directional antenna pattern with  $\lambda_B = 10^3$  BSs/km<sup>2</sup> to investigate the performance impact of BS antenna height on the coverage probability. From Fig.6, we can see that:

- For each antenna height, there exists an optimal antenna downtilt which can achieve the maximum coverage probability.
- The higher the BS antenna, the lower the coverage probability. This is because a larger  $L$  implies a tighter cap on the signal power and the interference power. In addition, a larger antenna height difference leads to a larger optimal antenna downtilt because  $\theta_b = \arctan\left(\frac{L}{r_b}\right)$  ( $r_b$  is the distance from the BS at point  $b$  to the typical UE).

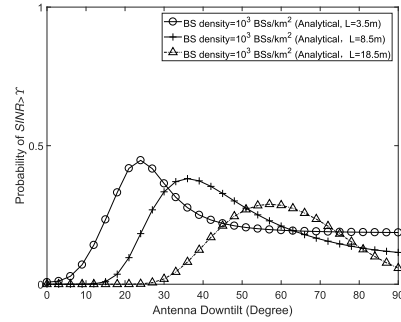


Fig. 6. The performance impact of BS antenna height on the coverage probability with  $\gamma = 0$  dB.

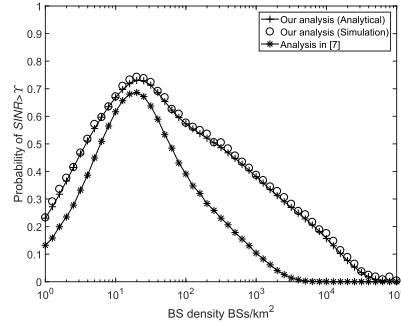


Fig. 7. Coverage probability vs. base station density with the optimal antenna downtilt and  $\gamma = 0$  dB.

### E. Network Performance With the Optimal Network-Wide Antenna Downtilt

In this subsection, we investigate the coverage probability and the ASE with the optimal antenna downtilt compared with the results in [2]. Here, the optimal network-wide antenna downtilt means adopting the optimal antenna downtilt for every BS in the network.

1) *The Coverage Probability With the Optimal Network-Wide Antenna Downtilt:* Fig.7 shows the coverage probability with the optimal antenna downtilt and without any downtilt. As we can observe from Fig.6:

- The antenna downtilt does not change the trend of the coverage probability, i.e., it first increases and then decreases to zero as BS density increases.
- The coverage probability performance with the optimal antenna downtilt is always better than that without antenna downtilt. The coverage probability reaches zero when the BS density is  $3 \times 10^4$  BSs/km<sup>2</sup>, while it is around  $3 \times 10^3$  BSs/km<sup>2</sup> in [7].

2) *The ASE With the Optimal Network-Wide Antenna Downtilt:* In the following, we present the ASE performance with the optimal antenna downtilt.

Fig.8 shows the ASE with and without optimal antenna downtilt. From Fig.8, we can draw the following observations:

- After using the optimal antenna downtilt, the ASE increases as BS density increases until  $2 \times 10^4$  BSs/km<sup>2</sup>, then it decreases to zero when BS density is around  $2 \times 10^5$  BSs/km<sup>2</sup>.
- The optimal antenna downtilt improves the ASE significantly and delay the ASE crash by nearly one order of magnitude in terms of the base station density.

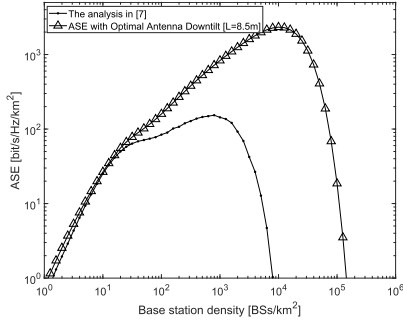


Fig. 8.  $A^{ASE}(\lambda, \gamma_0)$  vs. base station density with the optimal antenna downtilt and without antenna downtilt.

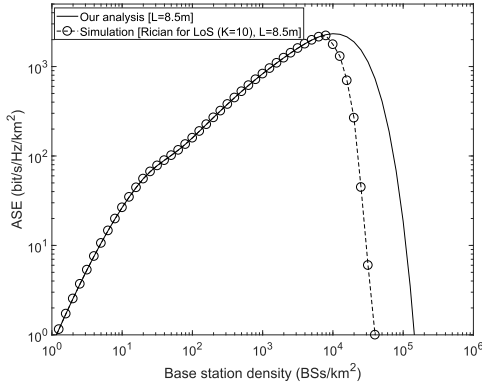


Fig. 9.  $A^{ASE}(\lambda, \gamma_0)$  vs base station density (Rayleigh fading for NLoS transmissions and Rician fading ( $K = 10$ ) for LoS transmissions with  $\gamma = 0$ dB).

3) *The Performance Impact of Rician Fading on the ASE With the Optimal Network-Wide Antenna Downtilt:* In Fig.9, we investigate the performance of coverage probability under the assumptions of Rayleigh fading for NLoS transmissions and Rician fading ( $K = 10$ ) for LoS transmissions. From Fig.9, we can see that Rician fading makes no difference when the BS density is smaller than  $8 \times 10^3$  BSs/km<sup>2</sup>, and then the ASE crash happens earlier than the case with Rayleigh fading. The intuition is that Rayleigh fading exhibits more channel fluctuation than Rician fading, and hence it can mildly combat the ASE Crash by providing an opportunistic channel gain to the signal power. However, such beneficial channel fluctuation is insignificant compared to the ASE Crash, which is caused by the physical limitation on capping the signal power.

## VI. CONCLUSION

In this paper, we investigated the impact of the 3D practical antenna pattern and downtilt on the performance of DL cellular networks. We show that there exists an optimal antenna downtilt to achieve the maximum coverage probability for each BS density. Analytical results were obtained for the optimal antenna downtilt and the coverage probability. Our results showed that there are three components determining the optimal antenna downtilt, and the optimal antenna downtilt increases as the BS density grows. Compared with [7], we found that using the optimal antenna downtilt can improve

the ASE performance significantly. Specifically, it can delay the ASE crash by nearly one order of magnitude in terms of the BS density. As our future work, we will consider the optimal antenna height with a multi-antenna setup in the cellular networks.

## APPENDIX A PROOF OF THEOREM 1

For clarity, we first summarize our ideas to prove Theorem 1. In order to evaluate  $p^{\text{cov}}(\lambda_B, \gamma)$ , the first key step is to calculate the distance PDFs for the events that the typical UE is associated with the strongest BS with a LoS path or that with a NLoS path, so that the integral of  $\Pr[\text{SINR} > \gamma]$  can be performed over the distance  $w$ . The second key step is to calculate  $\Pr[\text{SINR} > \gamma]$  for the LoS and the NLoS cases conditioned on  $w$  and  $\varphi_{\bar{b},1}$ . Since the two events that the typical UE is connected to a BS with a LoS path and that with a NLoS path are disjoint events, we have the probability of coverage  $p^{\text{cov}}(\lambda_B, \gamma)$  can be derived as

$$\begin{aligned}
 p^{\text{cov}}(\lambda_B, \gamma) &= \int_0^{\frac{\pi}{S}} \int_0^\infty \Pr \left[ \frac{P_B G(\varphi_{\bar{b},1}, \theta_b, \theta_{\text{tilt}}) \zeta(r) g}{I_{\text{agg}} + N_0} > \gamma \middle| r \right] \\
 &\quad \times f_R(r) f(\varphi) dr d\varphi \\
 &= \int_0^{\frac{\pi}{S}} \int_0^{\sqrt{d_1^2 - L^2}} \Pr \left[ \frac{P_B G(\varphi_{\bar{b},1}, \theta_b, \theta_{\text{tilt}}) \zeta_1^L(r) g}{I_{\text{agg}} + N_0} > \gamma \middle| r \right] \\
 &\quad \times f_{R,1}^L(r) f(\varphi) dr d\varphi \\
 &\quad + \int_0^{\frac{\pi}{S}} \int_0^{\sqrt{d_1^2 - L^2}} \Pr \left[ \frac{P_B G(\varphi_{\bar{b},1}, \theta_b, \theta_{\text{tilt}}) \zeta_1^{NL}(r) g}{I_{\text{agg}} + N_0} \right. \\
 &\quad \left. > \gamma \middle| r \right] \times f_{R,1}^{NL}(r) f(\varphi) dr d\varphi \\
 &\quad \vdots \\
 &\quad + \int_0^{\frac{\pi}{S}} \int_{\sqrt{d_{n-1}^2 - L^2}}^\infty \Pr \left[ \frac{P_B G(\varphi_{\bar{b},1}, \theta_b, \theta_{\text{tilt}}) \zeta_n^L(r) g}{I_{\text{agg}} + N_0} \right. \\
 &\quad \left. > \gamma \middle| r \right] \times f_{R,n}^L(r) f(\varphi) dr d\varphi \\
 &\quad + \int_0^{\frac{\pi}{S}} \int_{\sqrt{d_{n-1}^2 - L^2}}^\infty \Pr \left[ \frac{P_B G(\varphi_{\bar{b},1}, \theta_b, \theta_{\text{tilt}}) \zeta_n^{NL}(r) g}{I_{\text{agg}} + N_0} \right. \\
 &\quad \left. > \gamma \middle| r \right] \times f_{R,n}^{NL}(r) f(\varphi) dr d\varphi \\
 &= \sum_{n=1}^N (T_n^L + T_n^{NL}) \tag{35}
 \end{aligned}$$

where  $f_R(r)$  is the distance distributions of the signal link which can be divided to  $f_{R,n}^L(r)$  and  $f_{R,n}^{NL}(r)$ ,  $f_{R,n}^L(r)$  and  $f_{R,n}^{NL}(r)$  are the distance distribution of the n-piece signal link when the link is LoS and NLoS,  $I_{\text{agg}}$  is the aggregation interference from the LoS path and NLoS path.  $N_0$  is the additive white Gaussian noise (AWGN) power at each UE. In the following, we show how to compute  $f_{R,n}^L(r)$

in Eq.(35) first. To that end, we define three events as follows:

#### A. Event $B^L$

**The nearest BS with a LoS path and the horizontal arrive angle of the antenna  $\varphi_{\bar{b},1}$  to the typical UE, is located at distance  $R^L$ .** According to [14], the CCDF of  $R^L$  is written as  $\bar{F}_r^L(r) = \exp(-\int_0^r \text{Pr}_n^L(u) 2\pi u \lambda_B du)$ . Taking the derivative of  $(1 - \bar{F}_r^L(r))$  with regard to  $w$ , we can get the PDF of  $R^L$  as

$$f_r^L(r) = \exp\left(-\int_0^r \text{Pr}_n^L(u) 2\pi u \lambda_B du\right) \text{Pr}_n^L(u) 2\pi u \lambda_B. \quad (36)$$

#### B. Event $C^{NL}$ Conditioned on the Value of $R^L$

**Given that  $R^L = r$ , the typical UE is then associated with such BS at distance  $R^L = r$ .** To make the typical UE associated with the LoS BS at distance  $R^L = r$ , such BS should give the strongest average received power strength from such BS to the typical UE, i.e., there should be no BS with a NLoS path and the horizontal arrive angle of the antenna  $\varphi_{b_1,1}$  inside the disk centered on the UE with a radius of  $r_1 < r$  to outperform such LoS BS at distance  $R^L = r$ , where  $G(\varphi_{b_1,1}, \theta_{b_1}, \theta_{tilt}) \zeta^{NL}(w_1) = G(\varphi_{\bar{b},1}, \theta_{\bar{b}}, \theta_{tilt}) \zeta^L(w)$  and  $w_1 = \sqrt{r_1^2 + L^2}$ . BS at point  $b_1$  is located at the distance  $r_1$  to the typical UE. Such conditional probability of  $C^{NL}$  on the condition of  $R^L = r$  can be computed by

$$\text{Pr}[C^{NL} | R^L = r] = \exp\left(-\int_0^{r_1} (1 - \text{Pr}^L(u)) 2\pi u \lambda_B du\right). \quad (37)$$

#### C. Event $D^L$ Conditioned on the Value of $R^L$

**Given that  $R^{NL} = r$ , the typical UE is then associated with such BS at distance  $R^{NL} = r$ .** To make the typical UE associated with the LoS BS at distance  $R^L = r$ , there also should be no BS with a LoS path and the horizontal arrive angle of the antenna  $\varphi_{b_2,1}$  inside the disk centered on the UE with a radius of  $r_2 < r$  to outperform such LoS BS at distance  $R^L = r$ , where  $G(\varphi_{b_2,1}, \theta_{b_2}, \theta_{tilt}) \zeta^L(w_2) = G(\varphi_{\bar{b},1}, \theta_{\bar{b}}, \theta_{tilt}) \zeta^L(w)$  and  $w_2 = \sqrt{r_2^2 + L^2}$ . BS at point  $b_2$  is located at the distance  $r_2$  to the typical UE. Such conditional probability of  $D^L$  on the condition of  $R^{NL} = r$  can be computed by

$$\text{Pr}[D^L | R^L = r] = \exp\left(-\int_0^{r_2} \text{Pr}^L(u) 2\pi u \lambda_B du\right). \quad (38)$$

we can get the PDF of  $R^L$  as

$$f_R^L(r) = \text{Pr}[C^{NL} | R^L = r] \text{Pr}[D^L | R^L = r] f_r^L(r). \quad (39)$$

Considering the distance range of  $d_{n-1} < \sqrt{r^2 + L^2} < d_n$ , we can extract the segment of  $f_{R,n}^L(r)$  from  $f_R^L(r)$  as

$$\begin{aligned} f_{R,n}^L(r) &= \exp\left(-\int_0^{r_2} \text{Pr}_n^L(u) 2\pi u \lambda_B du\right) \\ &\times \exp\left(-\int_0^{r_1} (1 - \text{Pr}_n^L(u)) 2\pi u \lambda_B du\right) \\ &\times \exp\left(-\int_0^r \text{Pr}_n^L(u) 2\pi u \lambda_B du\right) \text{Pr}_n^L(u) 2\pi u \lambda_B. \end{aligned} \quad (40)$$

where

$$r_1^2 = \left(\frac{G(\varphi_{\bar{b},1}, \theta_{\bar{b}}, \theta_{tilt}) A_L}{G(\varphi_{b_1,1}, \theta_{b_1}, \theta_{tilt}) A_{NL}}\right)^{-\frac{2}{\alpha_{NL}}} (r^2 + L^2)^{\frac{\alpha_L}{\alpha_{NL}}}, \quad (41)$$

and

$$r_2^2 = \left(\frac{G(\varphi_{\bar{b},1}, \theta_{\bar{b}}, \theta_{tilt})}{G(\varphi_{b_2,1}, \theta_{b_2}, \theta_{tilt})}\right)^{-\frac{2}{\alpha_L}} (r^2 + L^2). \quad (42)$$

Having obtained  $f_{R,n}^L(r)$ , we move on to evaluate  $\text{Pr}[SINR > \gamma | w, \varphi_{\bar{b},1} | \text{LoS}]$  in Eq.(35) as

$$\begin{aligned} &\text{Pr}\left[\frac{P_B G(\varphi_{\bar{b},1}, \theta_r, \theta_{tilt}) \zeta_b^L(w) g_{\bar{b}}}{I_{agg} + N_0} > \gamma \mid w, \varphi_{\bar{b},1}\right] \\ &= \text{Pr}\left[g_{\bar{b}} > \frac{\gamma (I_{agg} + N_0)}{P_B G(\varphi_{\bar{b},1}, \theta_r, \theta_{tilt}) A^L (r^2 + L^2)^{-\frac{\alpha_L}{2}}} \mid w, \varphi_{\bar{b},1}\right] \\ &= \exp\left(-\frac{\gamma N_0}{P_B G(\varphi_{\bar{b},1}, \theta_r, \theta_{tilt}) A^L (r^2 + L^2)^{-\frac{\alpha_L}{2}}}\right) \mathcal{L}_{I_{agg}}^L(s), \end{aligned} \quad (43)$$

where  $I_{agg}$  is the aggregation interference from the LoS path and NLoS path.  $s = \frac{\gamma}{P_B G(\varphi_{\bar{b},1}, \theta_r, \theta_{tilt}) A^L w^{-\alpha_L}}$ ,

$$\begin{aligned} &\mathcal{L}_{I_{agg}}^L(s) \\ &= \mathbb{E}_{[I_{agg}]} \{\exp(-s I_{agg})\} \\ &= \mathbb{E}_{[\phi, \{g\}]} \left\{ \exp\left[-s \left( \sum_{i \in \phi_b/b} \sum_{n=1}^S P_B g_i \zeta_i G(\varphi_{i,n}, \theta_u, \theta_{tilt}) \right) \right] \right\} \\ &\quad + \sum_{n=2}^S P_B A^L (r^2 + L^2)^{-\frac{\alpha_L}{2}} G(\varphi_{b,n}, \theta_r, \theta_{tilt}) g \Bigg] \Bigg\} \\ &= \exp\left(-2\pi \lambda_B \int_0^{\frac{\pi}{s}} \int_r^\infty \left(1 - \mathbb{E}_{\{g\}} \left\{ \exp\left(-s \sum_{n=1}^s P_B \zeta(u) G(\varphi_{b,n}, \theta_u, \theta_{tilt})\right) \right\} \right) \right. \\ &\quad \left. \times u f(\varphi_{b,1}) du d\varphi_{b,1}\right) \\ &\quad \times \prod_{n=2}^S \mathbb{E}_{\{g\}} \left\{ \exp\left[P_B A^L (r^2 + L^2)^{-\frac{\alpha_L}{2}} G(\varphi_{b,n}, \theta_r, \theta_{tilt})\right] \right\} \\ &= \exp\left(-2\pi \lambda_B \int_0^{\frac{\pi}{s}} \int_r^\infty \left( \frac{u}{1 + (s \sum_{n=1}^s P_B \zeta(u) G(\varphi_{b,n}, \theta_u, \theta_{tilt}))^{-1}} du \right) \right. \\ &\quad \left. \times f(\varphi_{b,1}) d\varphi_{b,1}\right) \\ &\quad \times \prod_{n=2}^S \left( \frac{1}{P_B A^L (r^2 + L^2)^{-\frac{\alpha_L}{2}} G(\varphi_{b,n}, \theta_r, \theta_{tilt}) - 1} \right) \end{aligned} \quad (44)$$

where  $\theta_u = \arctan\left(\frac{L}{u}\right)$  is a function of  $u$ , when the antenna height difference is a constant and  $G(\varphi_{b,n}, \theta_u, \theta_{tilt})$

is a determined variable conditioned on  $\varphi_{b,1}$  and  $u$ . Similar to the process of LoS, we have omitted the proof steps of the computation of  $f_{R,n}^{NL}(r)$  in Eq.(35) and  $\Pr[SINR > \gamma | w, \varphi_{b,1} | \text{NLoS}]$  in Eq.(35) for brevity. Our proof is thus completed.

#### APPENDIX B PROOF OF THEOREM 4

In Theorem 1, the coverage probability can be written as Eq.(35). As  $\lambda_B, \gamma$  are constants, to get the derivative of  $p^{\text{cov}}(\lambda_B, \gamma)$  respect to  $\theta_{\text{tilt}}$ , we treat the antenna pattern gain in the horizontal direction as another independent variable. Except for the signal, the other factors which lead to the optimal antenna downtilt can be divided into the noise part  $\Omega_{\text{noise}}$ , the LoS interference part  $\Omega_{I_{\text{LoS}}}$  and the NLoS interference part  $\Omega_{I_{\text{NLoS}}}$ . Then we let the derivative of Eq.(35) be zero, thus all parts in Eq.(35) should be zero. Take the first part of Eq.(35) as an example,

$$\begin{aligned} p_1^{\text{cov}}(\lambda_B, \gamma) &= \int_0^{\frac{\pi}{6}} \int_0^{\sqrt{d_1^2 - L^2}} \exp\{\Omega_{\text{noise}} + \Omega_{I_{\text{LoS}}} + \Omega_{I_{\text{NLoS}}}\} \\ &\quad \times f_{R,1}^L(r) f(\varphi) dr d\varphi \end{aligned} \quad (45)$$

and

$$\int_0^{\sqrt{d_1^2 - L^2}} \{\Omega_{\text{noise}} + \Omega_{I_{\text{LoS}}} + \Omega_{I_{\text{NLoS}}}\}'_{\theta_{\text{tilt}}} f_{R,1}^L(r) dr = 0 \quad (46)$$

where

$$\begin{aligned} &\Omega_{I_{\text{LoS}}} + \Omega_{I_{\text{NLoS}}} + \Omega_{\text{noise}} \\ &= -2\pi\lambda_B \left( \int_r^{d_1} \frac{\text{Pr}_1^L(u)u}{1 + \frac{G(\varphi_{b,1}, \theta_r, \theta_{\text{tilt}})}{\gamma \sum_{n=1}^S G(\varphi_{b,n}, \theta_u, \theta_{\text{tilt}})} \left(\frac{u^2 + L^2}{r^2 + L^2}\right)^{\frac{\alpha_L}{2}}} du \right. \\ &\quad \left. + \int_{\sqrt{d_{n-1}^2 - L^2}}^{\infty} \frac{\text{Pr}_n^L(u)u}{1 + \frac{G(\varphi_{b,1}, \theta_r, \theta_{\text{tilt}})}{\gamma \sum_{n=1}^S G(\varphi_{b,n}, \theta_u, \theta_{\text{tilt}})} \left(\frac{u^2 + L^2}{r^2 + L^2}\right)^{\frac{\alpha_L}{2}}} du \right) \\ &\quad \vdots \\ &\quad - 2\pi\lambda_B \\ &\quad \times \left( \int_r^{d_1} \frac{(1 - \text{Pr}_1^L(u))u}{1 + \frac{G(\varphi_{b,1}, \theta_r, \theta_{\text{tilt}})A^L}{\gamma \sum_{n=1}^S A^{NL} G(\varphi_{b,n}, \theta_u, \theta_{\text{tilt}})} \left(\frac{u^2 + L^2}{r^2 + L^2}\right)^{\frac{\alpha_{NL}}{2}}} du \right. \\ &\quad \left. + \int_{\sqrt{d_{n-1}^2 - L^2}}^{\infty} \frac{(1 - \text{Pr}_n^L(u))u}{1 + \frac{G(\varphi_{b,1}, \theta_r, \theta_{\text{tilt}})A^L}{\gamma \sum_{n=1}^S A^{NL} G(\varphi_{b,n}, \theta_u, \theta_{\text{tilt}})} \left(\frac{u^2 + L^2}{r^2 + L^2}\right)^{\frac{\alpha_{NL}}{2}}} du \right) \\ &\quad - \frac{\gamma N_0}{\text{P}_B G(\varphi_{b,1}, \theta_r, \theta_{\text{tilt}}) A^L (r^2 + L^2)^{-\frac{\alpha_L}{2}}} \end{aligned} \quad (47)$$

which concludes our proof.

#### REFERENCES

- [1] *ArrayComm & William Webb*, Ofcom, London, U.K., 2007.
- [2] D. López-Pérez, M. Ding, H. Claussen, and A. H. Jafari, "Towards 1 Gbps/UE in cellular systems: Understanding ultra-dense small cell deployments," *IEEE Commun. Surveys Tuts.*, vol. 17, no. 4, pp. 2078–2101, 4th Quart., 2015.
- [3] X. Ge, S. Tu, G. Mao, C.-X. Wang, and T. Han, "5G ultra-dense cellular networks," *IEEE Wireless Commun.*, vol. 23, no. 1, pp. 72–79, Feb. 2016.
- [4] X. Zhang and J. G. Andrews, "Downlink cellular network analysis with multi-slope path loss models," *IEEE Trans. Commun.*, vol. 63, no. 5, pp. 1881–1894, May 2015.
- [5] T. Bai and R. W. Heath, Jr., "Coverage and rate analysis for millimeter-wave cellular networks," *IEEE Trans. Wireless Commun.*, vol. 14, no. 2, pp. 1100–1114, Feb. 2015.
- [6] M. Ding and D. López-Pérez, "Performance impact of base station antenna heights in dense cellular networks," *IEEE Trans. Wireless Commun.*, vol. 16, no. 12, pp. 8147–8161, Dec. 2017.
- [7] M. Ding, P. Wang, D. López-Pérez, G. Mao, and Z. Lin, "Performance impact of LoS and NLoS transmissions in dense cellular networks," *IEEE Trans. Wireless Commun.*, vol. 15, no. 3, pp. 2365–2380, Mar. 2016.
- [8] I. Atzeni, J. Arnau, and M. Kountouris, "Performance analysis of ultra-dense networks with elevated base stations," in *Proc. 15th Int. Symp. Modeling Optim. Mobile, Ad Hoc, Wireless Netw. (WiOpt)*, May 2017, pp. 1–6.
- [9] A. D. Gandhi, "Significant gains in coverage and downlink capacity from optimal antenna downtilt for closely-spaced cells in wireless networks," in *Proc. 23rd Wireless Opt. Commun. Conf. (WOCC)*, May 2014, pp. 1–6.
- [10] S. M. Razavizadeh, M. Ahn, and I. Lee, "Three-dimensional beamforming: A new enabling technology for 5G wireless networks," *IEEE Signal Process. Mag.*, vol. 31, no. 6, pp. 94–101, Nov. 2014.
- [11] *Further Advancements for E-UTRA Physical Layer Aspects (Release 9)*, document 3GPP TR 36.814, Mar. 2010.
- [12] H. C. Nguyen *et al.*, "Validation of tilt gain under realistic path loss model and network scenario," in *Proc. IEEE 78th Veh. Technol. Conf. (VTC Fall)*, Sep. 2013, pp. 1–5.
- [13] J. Fan, G. Y. Li, and X. Zhu, "Vertical beamforming with downtilt optimization in downlink cellular networks," in *Proc. IEEE Global Commun. Conf. (GLOBECOM)*, Dec. 2015, pp. 1–5.
- [14] J. G. Andrews, F. Baccelli, and R. K. Ganti, "A tractable approach to coverage and rate in cellular networks," *IEEE Trans. Commun.*, vol. 59, no. 11, pp. 3122–3134, Nov. 2011.
- [15] T. D. Novlan, H. S. Dhillon, and J. G. Andrews, "Analytical modeling of uplink cellular networks," *IEEE Trans. Wireless Commun.*, vol. 12, no. 6, pp. 2669–2679, Jun. 2013.
- [16] M. Ding and D. López-Pérez, "Please lower small cell antenna heights in 5G," in *Proc. IEEE Global Commun. Conf. (GLOBECOM)*, Dec. 2016, pp. 1–6.
- [17] M. Ding, D. López-Pérez, G. Mao, Z. Lin, and S. K. Das, "DNA-GA: A tractable approach for performance analysis of uplink cellular networks," *IEEE Trans. Commun.*, vol. 66, no. 1, pp. 355–369, Jan. 2018.
- [18] X. Ge, X. Tian, Y. Qiu, G. Mao, and T. Han, "Small-cell networks with fractal coverage characteristics," *IEEE Trans. Commun.*, vol. 66, no. 11, pp. 5457–5469, Nov. 2018.
- [19] A. M. Hunter, J. G. Andrews, and S. Weber, "Transmission capacity of ad hoc networks with spatial diversity," *IEEE Trans. Wireless Commun.*, vol. 7, no. 12, pp. 5058–5071, Dec. 2008.
- [20] M. Danneberg, J. Holfeld, M. Grieger, M. Amro, and G. Fettweis, "Field trial evaluation of UE specific antenna downtilt in an LTE downlink," in *Proc. Int. ITG Workshop Smart Antennas (WSA)*, Mar. 2012, pp. 274–280.
- [21] N. Seifi, M. Coldrey, M. Matthaiou, and M. Viberg, "Impact of base station antenna tilt on the performance of network MIMO systems," in *Proc. IEEE 75th Veh. Technol. Conf. (VTC Spring)*, May 2012, pp. 1–5.
- [22] M. Baianifar, S. Khavari, S. M. Razavizadeh, and T. Svensson, "Impact of user height on the coverage of 3D beamforming-enabled massive MIMO systems," in *Proc. IEEE 28th Annu. Int. Symp. Pers., Indoor, Mobile Radio Commun. (PIMRC)*, Oct. 2017, pp. 1–5.
- [23] S. K. Moghaddam and S. M. Razavizadeh, "Joint tilt angle adaptation and beamforming in multicell multiuser cellular networks," *Comput. Elect. Eng.*, vol. 61, pp. 195–207, Jul. 2017.
- [24] A. Fotouhi, M. Ding, and M. Hassan, "Flying drone base stations for macro hotspots," *IEEE Access*, vol. 6, pp. 19530–19539, 2018.

[25] X. Ge, B. Yang, J. Ye, G. Mao, C.-X. Wang, and T. Han, "Spatial spectrum and energy efficiency of random cellular networks," *IEEE Trans. Commun.*, vol. 63, no. 3, pp. 1019–1030, Mar. 2015.

[26] R. Zi, X. Ge, J. Thompson, C.-X. Wang, H. Wang, and T. Han, "Energy efficiency optimization of 5G radio frequency chain systems," *IEEE J. Sel. Areas Commun.*, vol. 34, no. 4, pp. 758–771, Apr. 2016.

[27] M. Ding, D. López-Pérez, and G. Mao. (Apr. 2017). "A new capacity scaling law in ultra-dense networks." [Online]. Available: <https://arxiv.org/abs/1704.00399v1>

[28] M. Ding, D. López-Pérez, G. Mao, P. Wang, and Z. Lin, "Will the area spectral efficiency monotonically grow as small cells go dense?" in *Proc. IEEE Global Commun. Conf. (GLOBECOM)*, Dec. 2015, pp. 1–7.

[29] *Small Cell Enhancements for E-UTRA and E-UTRAN—Physical Layer Aspects*, document 3GPP, TR 36.872, Dec. 2013.

[30] (2003). *Subsection 3.5.3, Spatial Channel Model Text Description V6.0 Spatial Channel Model AHG (Combined Ad-Hoc From 3GPP & 3GPP2)*. Online: Available: [http://www.3gpp.org/ftp/tsg\\_ran/WG1\\_RL1/3GPP\\_3GPP2\\_SCM/ConfCall-16-20030417/SCM-134%Text%v6.0.zip](http://www.3gpp.org/ftp/tsg_ran/WG1_RL1/3GPP_3GPP2_SCM/ConfCall-16-20030417/SCM-134%Text%v6.0.zip)

[31] *Further Enhancements to LTE Time Division Duplex (TDD) for Downlink-Uplink (DL-UL) Interference Management and Traffic Adaptation*, document 3GPP, TR 36.828, Jun. 2012.

[32] N. Seifi, R. W. Heath, Jr., M. Coldrey, and T. Svensson, "Adaptive multicell 3-D beamforming in multi-antenna cellular networks," *IEEE Trans. Veh. Technol.*, vol. 65, no. 8, pp. 6217–6231, Aug. 2016.

[33] X. Li, T. Bai, and R. W. Heath, Jr., "Impact of 3D base station antenna in random heterogeneous cellular networks," in *Proc. IEEE Wireless Commun. Netw. Conf. (WCNC)*, Apr. 2014, pp. 2254–2259.

[34] F. Gunnarsson *et al.*, "Downtilted base station antennas—A simulation model proposal and impact on HSPA and LTE performance," in *Proc. IEEE 68th Veh. Technol. Conf.*, Sep. 2008, pp. 1–5.



**Junnan Yang** (S'17) received the B.Eng. degree in electronics engineering and the M.Sc. degree in mechanical engineering from Zhejiang University, Zhejiang, China, in 2012 and 2015, respectively. He is currently pursuing the Ph.D. degree in engineering with the University of Technology Sydney. His research interests include 5G wireless communication networks, stochastic geometry, dense cellular networks, network performance analysis, intelligent transport systems, and applied graph theory and its applications in telecommunications.



**Ming Ding** (M'12–SM'17) received the B.S. and M.S. degrees (Hons.) in electronics engineering and the Ph.D. degree in signal and information processing from Shanghai Jiao Tong University, Shanghai, China, in 2004, 2007, and 2011, respectively. From 2007 to 2014, he was a Researcher/Senior Researcher/Principal Researcher with Sharp Laboratories of China, Shanghai. He was the Algorithm Design Director and the Programming Director of a system-level simulator of future telecommunication networks with Sharp Laboratories of China for more than seven years. He is currently a Senior Research Scientist with Data61, CSIRO, Sydney, NSW, Australia. He has authored over 80 papers in IEEE journals and conferences, all in recognized venues, and about 20 3GPP standardization contributions and a Springer book *Multi-point Cooperative Communication Systems: Theory and Applications*. He holds 16 U.S. patents and co-invented another 100+ patents on 4G/5G technologies in CN, JP, and EU. He was awarded as the Exemplary Reviewer for the IEEE TRANSACTIONS ON WIRELESS COMMUNICATIONS in 2017. He was the Lead Speaker of the industrial presentation on unmanned aerial vehicles at the IEEE Globecom 2017, which was awarded as the Most Attended Industry Program in the conference. He is currently an Editor of the IEEE TRANSACTIONS ON WIRELESS COMMUNICATIONS. He is a guest editor/co-chair/co-tutor/TPC member of several IEEE top-tier journals/conferences, e.g., the IEEE JOURNAL ON SELECTED AREAS IN COMMUNICATIONS, the *IEEE Communications Magazine*, and the IEEE Globecom Workshops.



**Guoqiang Mao** (S'98–M'02–SM'08–F'18) was with the School of Electrical and Information Engineering, The University of Sydney. In 2014, he joined the University of Technology Sydney as a Professor of wireless networking and the Director of the Center for Real-Time Information Networks. He has published over 200 papers in international conferences and journals, which have been cited more than 7000 times. His research interests include intelligent transport systems, applied graph theory and its applications in telecommunications, the Internet of Things, wireless sensor networks, wireless localization techniques, network modeling, and performance analysis. He is a fellow of IET. He was a recipient of the Top Editor Award for outstanding contributions to the IEEE TRANSACTIONS ON VEHICULAR TECHNOLOGY in 2011, 2014, and 2015. He has been an Editor of the IEEE TRANSACTIONS ON INTELLIGENT TRANSPORTATION SYSTEMS since 2018, the IEEE TRANSACTIONS ON WIRELESS COMMUNICATIONS since 2014, and the IEEE TRANSACTIONS ON VEHICULAR TECHNOLOGY since 2010. He is a Co-Chair of the IEEE Intelligent Transport Systems Society Technical Committee on Communication Networks. He has served as the chair, a co-chair, and a TPC member for a number of international conferences.



**Zihuai Lin** (S'98–M'06–SM'10) received the Ph.D. degree in electrical engineering from the Chalmers University of Technology, Sweden, in 2006. He held positions with Ericsson Research, Stockholm, Sweden. He was a Research Associate Professor with Aalborg University, Denmark. He is currently with the School of Electrical and Information Engineering, The University of Sydney, Australia. His research interests include source/channel/network coding, coded modulation, multi-in multi-out, OFDMA, SC-FDMA, radio resource management, cooperative communications, small-cell networks, 5G cellular systems, and the Internet of Things.



**De-Gan Zhang** (M'01) was born in 1969. He received the Ph.D. degree from Northeastern University, China. He is currently a Professor with the Tianjin Key Lab of Intelligent Computing and Novel Software Technology, Key Lab of Computer Vision and System, Ministry of Education, Tianjin University of Technology, Tianjin, China. His research interests include ITS, WSN, and the Internet of Things. He has been a member of the IEEE since 2001.



**Tom H. Luan** received the B.E. degree in electrical and computer engineering from Xi'an Jiaotong University, China, in 2004, the master's degree in electrical and computer engineering from the Hong Kong University of Science and Technology, Hong Kong, in 2007, and the Ph.D. degree in electrical and computer engineering from the University of Waterloo, Canada, in 2012. During 2013–2017, he was a Lecturer of mobile and apps with Deakin University, Australia. Since 2017, he has been a Professor with the School of Cyber Engineering, Xidian University, China. His researches mainly focus on the content distribution and media streaming in vehicular ad hoc networks and peer-to-peer networking, and protocol design and performance evaluation of wireless cloud computing and edge computing.